Supporting Information

Filter-feeding bivalves store and biodeposit colloidally stable gold nanoparticles

Matthew S. Hull[1,2,3], Perrine Chaurand[3,4], Jerome Rose[3,4], Melanie Auffan[3,4], Jean-Yves Bottero[3,4], Jason C. Jones[1,2], Irvin R. Schultz[5], Peter J. Vikesland[1,2,3]*

[1]Virginia Tech Department of Civil and Environmental Engineering, Blacksburg, Virginia, USA

[2] Virginia Tech Institute for Critical Technology and Applied Science (ICTAS)

[3]Center for the Environmental Implications of Nanotechnology (CEINT)

[4]CEREGE, UMR 6635 CNRS/Aix-Marseille University, International Consortium for the Environmental Implications of Nanotechnology (iCEINT), Aix-en-Provence, France

[5]Pacific Northwest National Laboratory, Marine Sciences Laboratory, Sequim, Washington, USA

AUTHOR EMAIL ADDRESS. pvikes@vt.edu

Characterization

Analysis of TEM images indicated that mean primary particle diameters were 7.8 ± 3.3, 15 ± 6.8, and 46 ± 5.3 nm (Table S1). Corresponding hydrodynamic diameters (Z_{ave}, nm) measured by dynamic light scattering (DLS) were 12.9 ± 0.4, 31.9 ± 0.3, and 44.1 ± 0.1 nm, respectively. Polydispersity indices ranged from 0.230 to 0.289, suggesting that suspensions were similarly monodisperse. Particle diameters predicted from the position of the surface plasmon resonance (SPR) band[1] were 4.2, 11.4, and 38.4 nm, which is in general agreement with the diameters measured by TEM and DLS. All particles were negatively charged at the pH of the assay (pH = 7.8) with electrophoretic mobilities of -1.47 ± 0.25, -2.05 ± 0.13, and -1.71 ± 0.01 μm-cm $(V\text{-}s)^{-1}$ for the 7.8, 15, and 46 nm BSA-AuNP, respectively. Accurate zeta potential values could not be calculated for these particles due to the soft BSA coating,[2, 3] nonetheless, these electrophoretic mobilities support the contention that the particles were negatively charged under the assay conditions.

Consideration of Dosimetry: Mass, Particle Number, and Surface Area

On a mass basis, approximately 70-80% of the 15 and 46 nm BSA-AuNP were removed from suspension after 180 h, compared to less than 40% of the 7.8 nm BSA-AuNP. In terms of particle number concentration, however, the number of 7.8 nm BSA-AuNP removed from suspension exceeded the number of 15 and 46 nm particles by 1.0×10^{14} and 1.5×10^{14} particles-mL^{-1}, respectively. When the concentrations are expressed in terms of the total surface area of particles removed, cumulative clearance of 7.8 and 15 nm BSA-AuNP were similar at approximately 3.0×10^{7} m^2-mL^{-1}, which was nearly three-fold greater than the total surface area concentration of the 46 nm BSA-AuNP removed.

Experimental Replication of Size-selective Biopurification of BSA-AuNP

It is worth noting that the SPR shift of ~4 nm could be replicated experimentally by preparing cocktails corresponding to the measured gold concentrations and predicted particle size distributions at t_0 and t_{120} during the size-selective uptake assay (Supporting Information Figure S7).

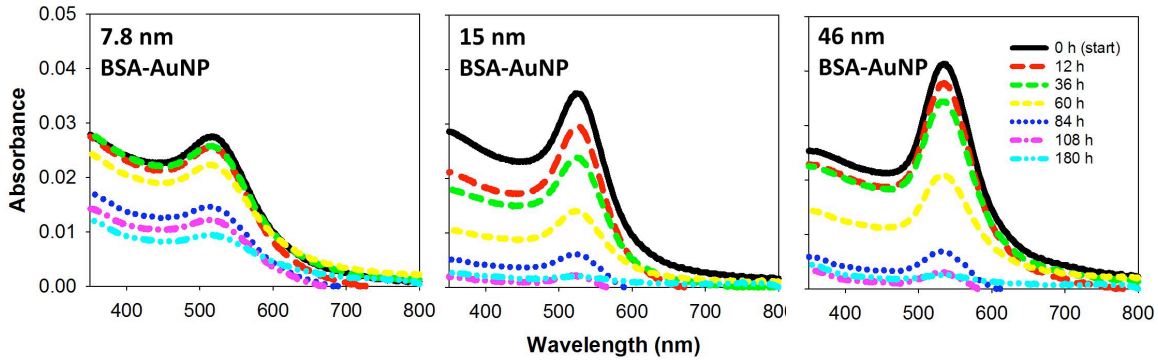

Figure S1. Plots of UV-Vis spectra showing the time-dependent (0 to 180 h) decrease in absorbance intensity at Abs_{SPR} for 7.8 nm, 15 nm, and 46 nm BSA-AuNP suspensions in the presence of *C. fluminea*. Initial concentrations of BSA-AuNP were mass normalized to 2 mg L^{-1} as [Au].

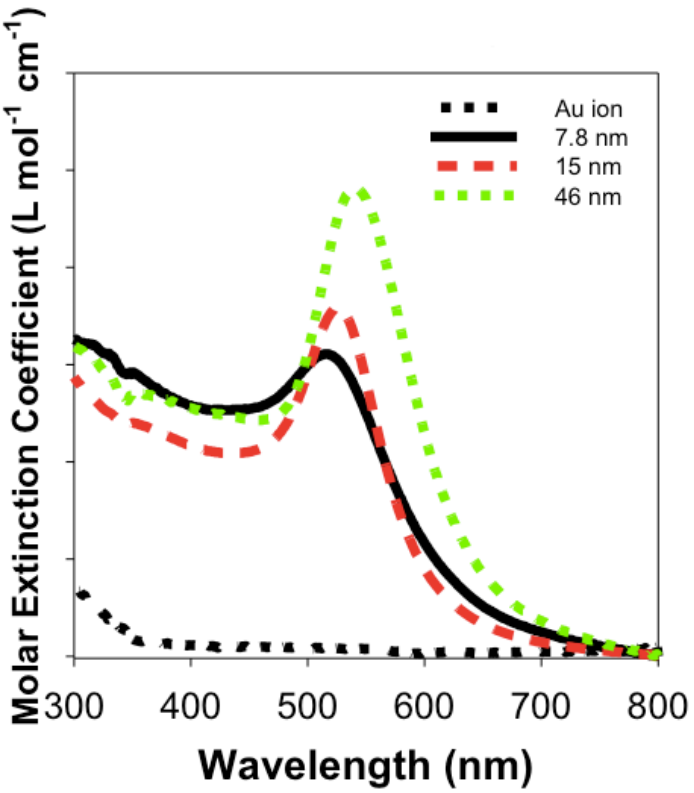

Figure S2. Extinction spectra for the Au ion and 7.8, 15, and 46 nm gold nanoparticles.

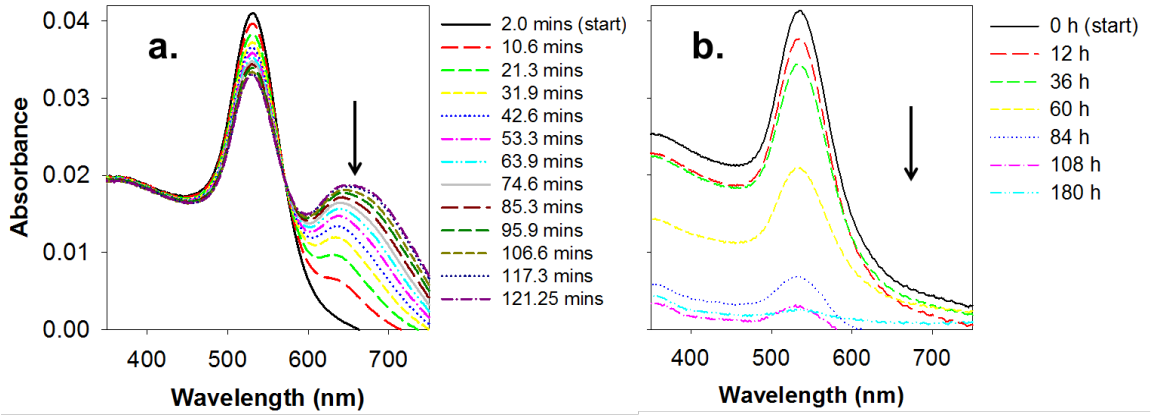

Figure S3. Characteristic changes in absorbance spectra and the location or height of Abs_{SPR} over time due to (a) aggregation in EPA MHS after 120 min versus (b) particle clearance by a filter-feeding bivalve. The arrow denotes the location of a new absorption band that forms upon aggregation of AuNP, but is not evident when AuNP are cleared from suspensions via biological filtration.

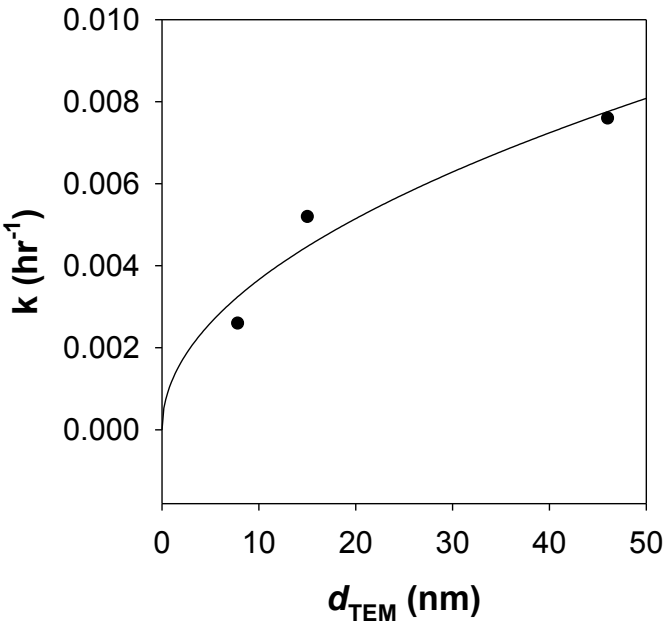

Figure S4. Plot showing first-order rate constants for clearance of BSA-AuNP as a function of primary particle diameter.

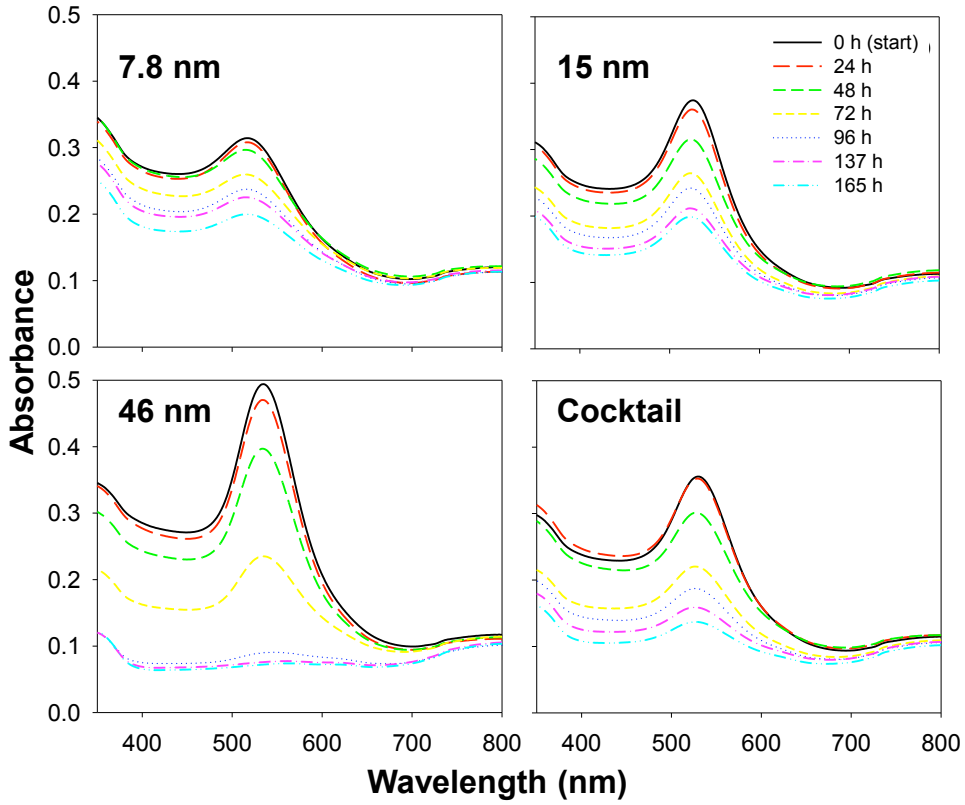

Figure S5. UV-Vis spectra showing the time-dependent decrease in absorbance intensity of the SPR band of three sizes of BSA-AuNP—prepared individually and in combination as a '*cocktail*' at a concentration of 15 mg L^{-1} as [Au]—in the presence of *C. fluminea*.

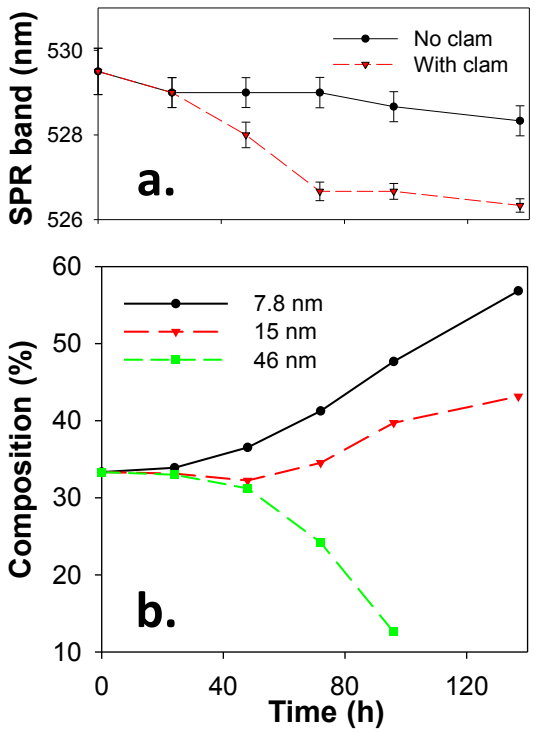

Figure S6. (a) Plot of the mean blue shift ± SD (n = 3) observed for the SPR band of the cocktail in the presence and absence of clams and (b) the predicted change in the respective contributions of each size of particle to the overall composition of the cocktail based on the size-dependent clearance rates. Beyond 96 h, the composition of 46 nm BSA-AuNP was below detection limits.

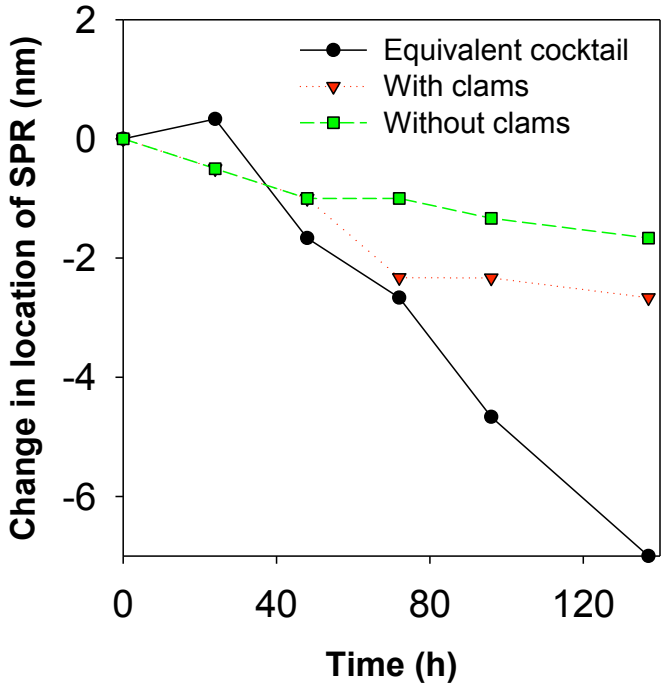

Figure S7. Comparison of average SPR band shift for BSA-AuNP cocktails from the size-selective uptake experiment (with and without clams) and the experiment with cocktails prepared at the particle size composition and total [Au] predicted from the size-selective uptake experiment.

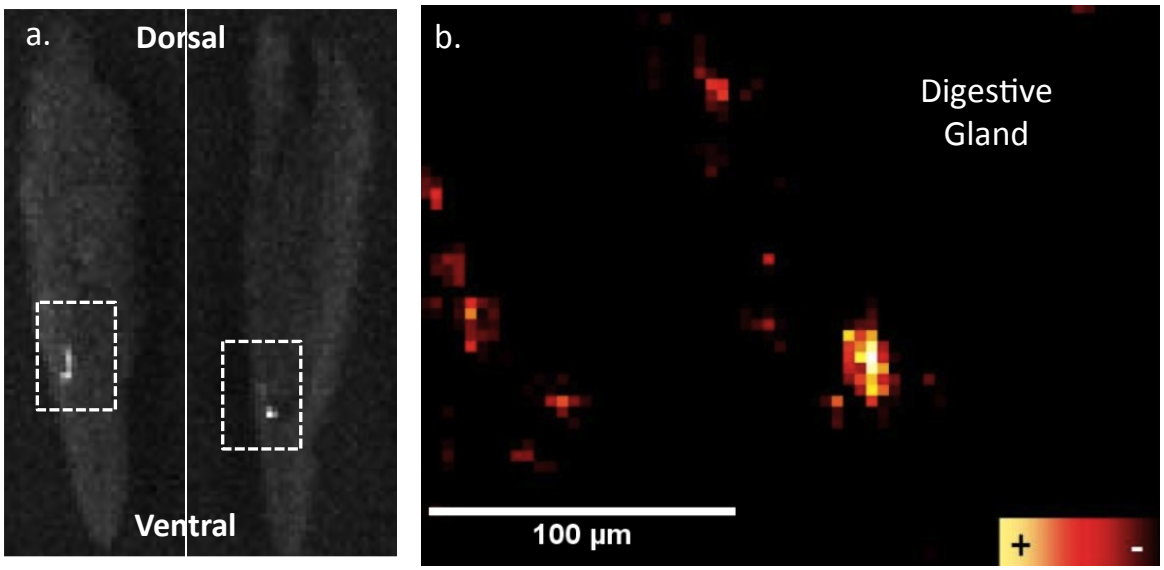

Figure S8. (a) μ-XRF image of *C. fluminea* tissue cross-sections showing the internalization of Au (light areas surrounded by dashed boxes) within the digestive tract; (b) synchrotron-based μ-XRF (LUCIA beamline) Au map of a cross-section of the *C. fluminea* digestive gland.

Table S1. Characteristics of BSA-AuNP. Size of primary particles on a TEM grid (n ≥ 100) is expressed as the median value of the size determined using ImagePro and as the diameter predicted by Haiss et al. using the location and height of the surface Plasmon resonance (SPR) band.[1] Mean effective hydrodynamic diameter (Z_{ave}, nm), polydispersity index (PDI), electrophoretic mobility (μm cm $(Vs)^{-1}$), and location of the SPR band as measured in EPA moderately hard reconstituted water (EPA MHS).

BSA-AuNP Suspension	TEM (nm)	Predicted by Haiss et al. (nm)	Z_{ave} (nm)	PDI	Electrophoretic mobility (μm cm $(Vs)^{-1}$)	SPR band (nm)
8 nm	7.8 ± 3.3	4.2	12.9 ± 0.4	0.23 ± 0.03	-1.06 ± 0.45	518
15 nm	15 ± 6.8	11	31.9 ± 0.3	0.24 ± 0.00	-1.96 ± 0.19	523
46 nm	46 ± 5.3	38	44.1 ± 0.1	0.29 ± 0.00	-1.80 ± 0.07	536

References

1. Haiss, W.; Thanh, N.; Aveyard, J.; Fernig, D., Determination of size and concentration of gold nanoparticles from UV-Vis spectra. *Anal Chem* **2007,** 79, 4215-4221.

2. Ohshima, H., Electrophoretic mobility of soft particles. *Journal of Colloid and Interface Science* **1994,** 163 (2), 474-483.

3. Ohshima, H., Electrophoresis of soft particles. *Adv Colloid Interface* **1995,** 62 (2-3), 189-235.